

# ERp44, a novel endoplasmic reticulum folding assistant of the thioredoxin family

Tiziana Anelli, Massimo Alessio, Alexandre Mezghrani, Thomas Simmen, Fabio Talamo, Angela Bachi and Roberto Sitia<sup>1,2</sup>

DiBiT-HSR and <sup>1</sup>Università Vita-Salute San Raffaele, Via Olgettina 58, I-20132 Milan, Italy

<sup>2</sup>Corresponding author  
e-mail r.sitia@hsr.it

T.Anelli and M.Alessio contributed equally to this work

**In human cells, Ero1-L $\alpha$  and -L $\beta$  (hEROs) regulate oxidative protein folding by selectively oxidizing protein disulfide isomerase. Specific protein–protein interactions are probably crucial for regulating the formation, isomerization and reduction of disulfide bonds in the endoplasmic reticulum (ER). To identify molecules involved in ER redox control, we searched for proteins interacting with Ero1-L $\alpha$ . Here, we characterize a novel ER resident protein (ERp44), which contains a thioredoxin domain with a CRFS motif and is induced during ER stress. ERp44 forms mixed disulfides with both hEROs and cargo folding intermediates. Whilst the interaction with transport-competent Ig-K chains is transient, ERp44 binds more stably with J chains, which are retained in the ER and eventually degraded by proteasomes. ERp44 does not bind a short-lived ribophorin mutant lacking cysteines. Its overexpression alters the equilibrium of the different Ero1-L $\alpha$  redox isoforms, suggesting that ERp44 may be involved in the control of oxidative protein folding.**

**Keywords:** endoplasmic reticulum/isomerase/oxidative protein folding/redox control/unfolded protein response

## Introduction

Proteins destined for the exocytic pathway or for the extracellular space are cotranslationally translocated into the endoplasmic reticulum (ER). In this organelle, they undergo several post-translational modifications, while being subject to stringent quality control, ensuring that only molecules that have attained their correct three-dimensional structure are transported to the Golgi (Ellgaard *et al.*, 1999). Proteins that fail to fold or assemble are eventually degraded, generally by cytosolic proteasomes (Klausner and Sitia, 1990; Kopito, 1997). The accumulation of unfolded proteins in the ER activates a signalling pathway known as the unfolded protein response (UPR), which leads to increased transcription of ER folding and quality control factors and transient inhibition of protein synthesis (Mori, 2000; Travers *et al.*, 2000). Regulatory elements have been identified in both

yeast and mammalian cells [the unfolded protein response element (UPRE) and ER stress elements (ERSEs), respectively] that mediate transcriptional induction (Kohno *et al.*, 1993; Mori *et al.*, 1998; Yoshida *et al.*, 1998; Roy and Lee, 1999).

Formation of disulfide (SS) bonds is essential for the folding and biological activity of many secreted and membrane proteins. In eukaryotes, oxidative protein folding takes place in the ER, under the assistance of many chaperones and oxidoreductases (PDI, ERp72, ERp57, etc.). Extensive isomerization of disulfide bonds is often required for complex proteins to attain their native structure. Moreover, certain disulfide bonds are reduced before the dislocation of aberrant proteins to the cytosol for proteasomal destruction (Tortorella *et al.*, 1998; Fagioli *et al.*, 2001). Therefore, excessive oxidation might lead to protein accumulation and aggregation in the ER, with severe consequences for the cell (Kopito and Ron, 2000). Cascades of protein–protein interactions probably allow the coexistence in the ER of disulfide isomerization and reduction with a powerful oxidative pathway (Debarbieux and Beckwith, 1999; Frand *et al.*, 2000; Tu *et al.*, 2000; Mezghrani *et al.*, 2001).

One of the key players in the control of disulfide bond formation is protein disulfide isomerase (PDI), an abundant ER oxidoreductase (Bulleid and Freedman, 1988). PDI donates oxidative equivalents to cargo proteins via the formation of mixed disulfides (Molinari and Helenius, 1999; Mezghrani *et al.*, 2001). To be effective in catalysing SS bond formation, PDI must be continuously re-oxidized. In both yeast and mammalian cells, members of the Ero1 family serve this function (Frand and Kaiser, 1999; Tu *et al.*, 2000; Mezghrani *et al.*, 2001). Human Ero1-L $\alpha$  and Ero1-L $\beta$  (hEROs) are ER luminal glycoproteins (Cabibbo *et al.*, 2000; Pagani *et al.*, 2000) that form mixed disulfides with PDI (Benham *et al.*, 2000; Mezghrani *et al.*, 2001). Whilst most cell types constitutively express Ero1-L $\alpha$ , human Ero1-L $\beta$  is induced during the UPR (Pagani *et al.*, 2000). Both hEROs accelerate oxidative folding of immunoglobulin (Ig) subunits, facilitating the re-oxidation of PDI (Mezghrani *et al.*, 2001). Yeast Ero1p has been shown to bind flavin adenine dinucleotide (Tu *et al.*, 2000), but the ultimate electron acceptor(s) in this ER disulfide bond formation pathway remain to be identified. In addition to mixed disulfides with PDI and other unidentified proteins, several monomeric Ero1-L $\alpha$  redox isoforms (OX1, OX2 and R) can be detected in transfected mammalian cells (Benham *et al.*, 2000). OX1 and OX2 could be part of a working cycle in which Ero1-L $\alpha$  adopts different conformations so as to capture electrons from PDI and donate them to upstream components in the pathway more efficiently.

To gain more information of the molecular machines controlling oxidative folding in human cells, we decided to

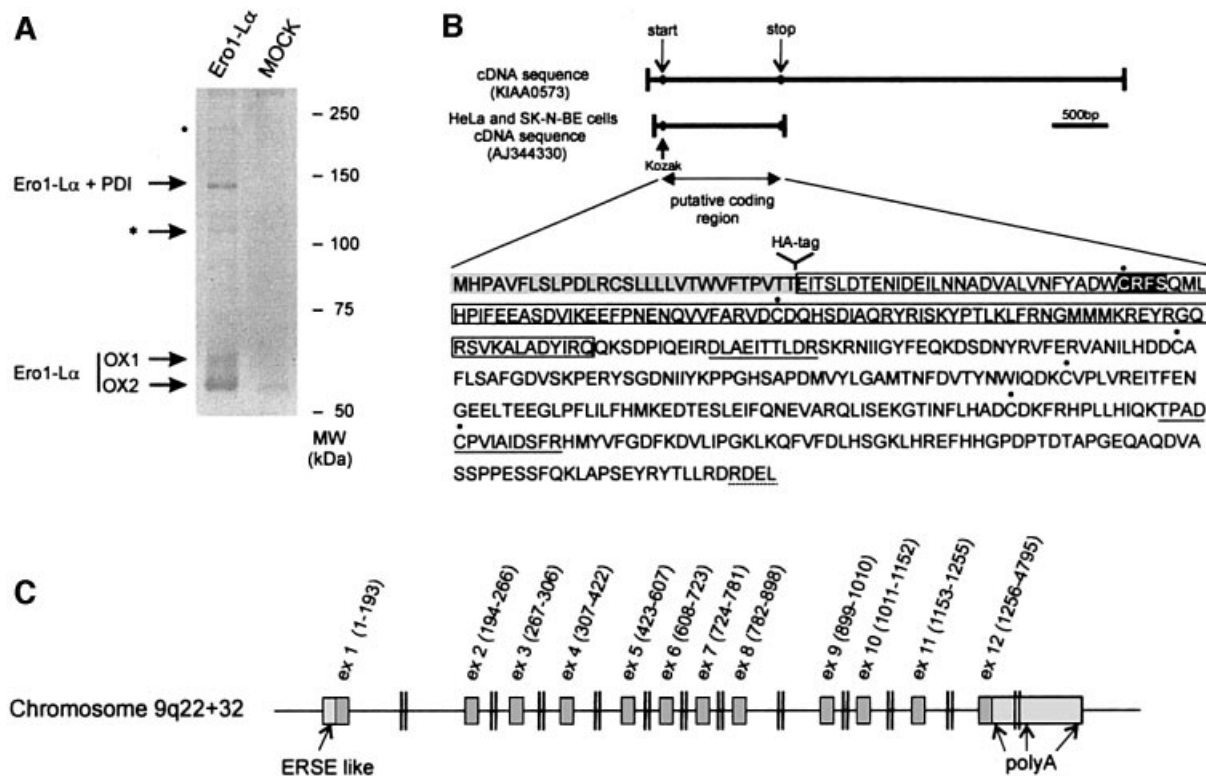


**Fig. 1.** Characterization of a novel protein forming mixed disulfides with Ero1- $\alpha$ . (A) Anti-myc immunoprecipitates from  $10^7$  HeLa cells stably transfected with a vector driving the expression of myc-tagged Ero1- $\alpha$  (Ero1- $\alpha$ ) or with an empty vector (MOCK) were resolved by SDS-PAGE under non-reducing conditions, and stained with Coomassie Blue colloidal. Bands were excised and analysed by MS. The band denoted by an asterisk was shown to contain peptides derived from Ero1- $\alpha$  and from an open reading frame, corresponding to KIAA0573, subsequently resequenced from HeLa and SK-N-BE cDNAs. The faint band indicated by a dot was excised and was shown by MS to contain the same peptides as were found in the band indicated by the asterisk. (B) Sequence of the 44 kDa protein forming mixed disulfides with Ero1- $\alpha$ . The two peptides sequenced in the mixed disulfide with Ero1- $\alpha$  are underlined. Note the presence of a N-terminal hydrophobic sequence (shaded), which is absent in the mature protein, and an RDEL motif at the C-terminus (underlined). The six cysteine residues are indicated by dots. The trx-like domain is boxed. The CRFS motif has a black background. (C) Chromosomal organization of the gene encoding ERp44 in humans. Note the presence of an ERSE-like sequence upstream of the translation initiation site.

characterize proteins that interact covalently with hEROs. Using tagged Ero1- $\alpha$  as bait, proteins were co-immunoprecipitated and identified by mass spectrometry (MS) and microsequencing. Here, we report the functional characterization of a novel UPR-induced ER resident protein (ERp44) that forms mixed disulfides with both hEROs, as well as with partially unfolded Ig subunits. Our results identify ERp44 as a novel ER resident folding assistant that may regulate the function of hEROs.

## Results

### Identification of a novel protein forming mixed disulfides with Ero1- $\alpha$

Stable HeLa transfectants expressing a myc-tagged human Ero1- $\alpha$  were lysed and immunoprecipitated with immobilized anti-myc antibodies. In addition to the two Ero1- $\alpha$  redox isoforms, OX1 and OX2 described previously (Benham *et al.*, 2000), several high-molecular weight bands were detectable in Ero1- $\alpha$  transfectants but not in mock-transfected cells (Figure 1A). The most abundant band was shown to contain both Ero1- $\alpha$  and PDI by western blotting and MS, confirming our previous findings (Benham *et al.*, 2000; Mezghrani *et al.*, 2001). A second

band, of ~110 kDa (indicated by an asterisk), was excised and analysed by MALDI peptide mass mapping and NanoES MS/MS, after in-gel tryptic digestion. In addition to eight peptides deriving from Ero1- $\alpha$  (covering 14% of the sequence with a mass accuracy within 40 p.p.m.), we identified nine additional peptides corresponding to a single ORF present in the human EST KIAA0573 (Kazusa DNA Research Institute, Kisarazu, Chiba, Japan). The nine peptides covered 21% of the KIAA0573 putative coding sequence, with a mass accuracy within 40 p.p.m. To confirm the identification, tandem MS experiments were performed on the unseparated peptide mixture. Of the five peptides fully sequenced, two (DLAEITTLDR and TPADCPVIAIDFR) unambiguously identified sequences encoded within KIAA0573 (underlined in Figure 1B). The remaining three (LLESYFR, FDGILTEGEGPR and LIANMPESGPSYEFHLTR) derived from Ero1- $\alpha$ , thus confirming the presence of both proteins in the 110 kDa band.

The portion of EST KIAA0573 containing the open reading frame was entirely resequenced from cDNAs obtained from HeLa and SK-N-BE cells, and the sequence submitted to the DDBJ/EMBL/GenBank database under accession number AJ344330 (Figure 1B). An ATG codon

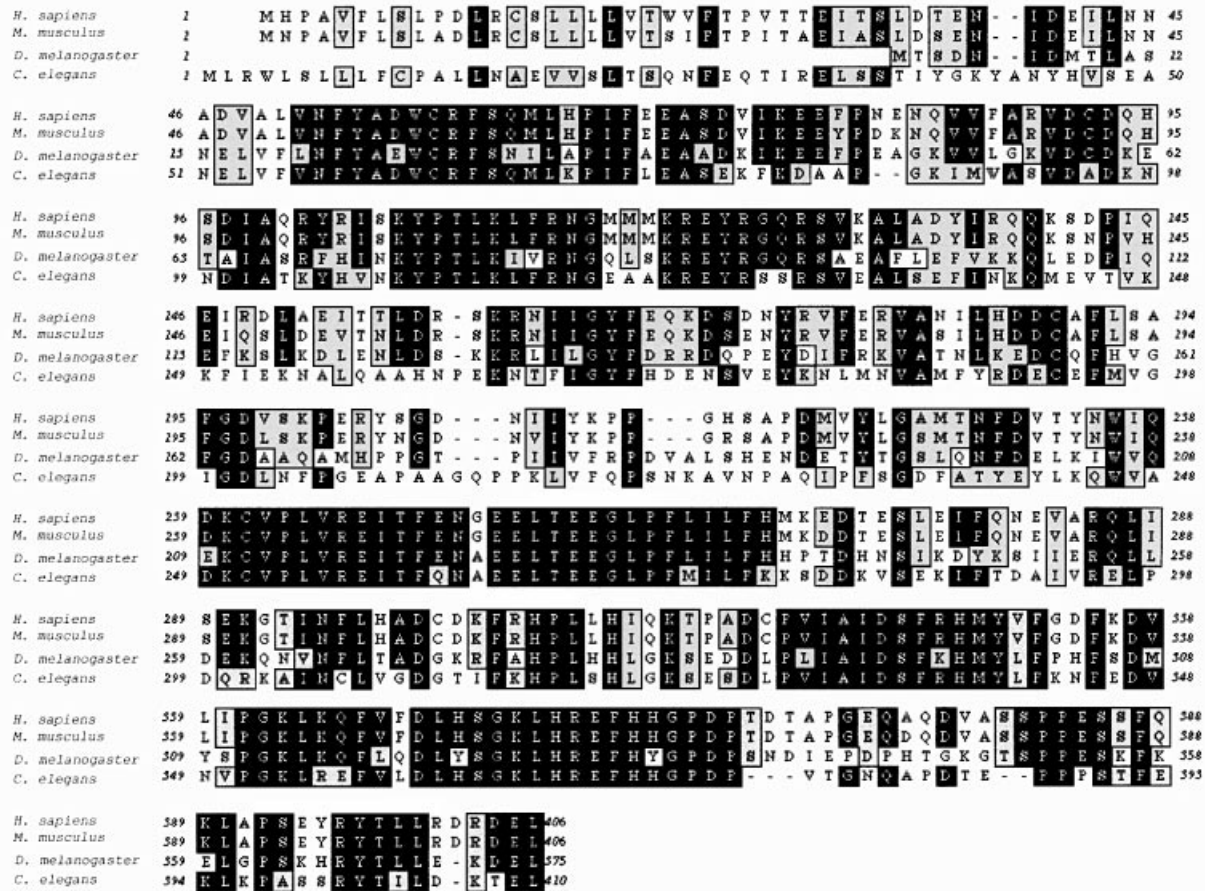


**Fig. 2.** Evolutionary conservation of ERp44. The sequences of ERp44-related polypeptides from *M.musculus* (18 day embryo cDNA, accession No. AK003217), *D.melanogaster* (alt1, accession No. AE003501), *C.elegans* (hypothetical protein C30H7.2, accession No. T25574). The alignment was performed using the pileup algorithm of the Wisconsin Package version 9.0, Genetics Computer Group (GCG; Madison, WI). Black boxes indicate identity and grey similarity.

within a proper initiation context (Kozak, 1997) and an in-frame termination codon were found, predicting a protein of 436 amino acids.

#### **ERp44 contains thioredoxin- and caseinase-like domains and a C-terminal ER localization motif**

SignalP computational analysis (Nielsen *et al.*, 1997) predicted an ER targeting signal sequence (von Heijne, 1989) with a cleavage site between Thr29 and Glu30 of the precursor protein (Figure 1B). Cleavage of the signal sequence was confirmed by MS analysis of the 110 kDa band, which revealed the presence of a peptide whose mass could only correspond to a Glu–Arg 30mer generated by leader cleavage and tryptic digestion (mass accuracy 20 p.p.m. after internal calibration). After cleavage, a molecular weight of 43.9 kDa is predicted for this Ero1- $\alpha$ -associated protein, which will be referred to hereafter as ERp44.

After the hydrophobic N-terminal sequence, a 109 residue domain homologous to thioredoxin (trx) is present. Computer modelling (Guex and Peitsch, 1997) reveals remarkable structural similarities to the trx-like domains of PDI and other members of the trx family (not shown). Of note, however, is that the second cysteine in the canonical CXXC motif is replaced by a serine, yielding the sequence CRFS.

The trx-like domain is followed by a 62 amino acid stretch displaying weaker similarities with the second domain of caseinase. After a long sequence with no obvious sequence homologies with other proteins, the polypeptide ends with the tetrapeptide RDEL, shown previously to mediate ER localization (Andres *et al.*, 1990).

#### **Genomic organization and evolutionary conservation of ERp44**

*In silico* BLAST searches of the working draft sequence of the human genome ([www.ncbi.nlm.nih.gov](http://www.ncbi.nlm.nih.gov)) allowed the mapping of ERp44 on chromosome 9q22+32 (genomic contig NT\_008513). The coding sequence appears to be encoded within 12 exons (Figure 1C). The first four exons encode the leader peptide and trx-like domain, whilst the region displaying homologies with caseinase is encoded within exon 5. The last exon encodes the 3' UTR, with three clusters of potential poly(A) addition sequences at positions 1414–1525, 2652–2866 and 4764 in the KIAA0573 cDNA.

As shown in Figure 2, ERp44 homologues are present in *Mus musculus* (89% sequence identity), *Drosophila melanogaster* (alt1, 51% identity), *Caenorhabditis elegans* (hypothetical protein C30H7.2, 45% identity). Interestingly, all the homologous genes share a CRFS motif in the

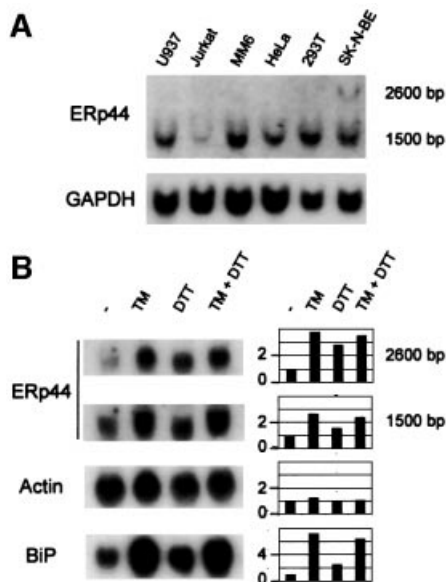


**Fig. 3.** ERp44 transcripts are widely expressed in human cell lines and can be further induced by ER stress. (A) Northern blot analyses were performed on total RNA extracted from the cell lines indicated, obtained from ATCC. Blots were hybridized sequentially with probes specific for ERp44 (top panel) or GAPDH (bottom panel) for normalization. (B) ERp44 transcripts accumulate during the UPR. SK-N-BE neuroblastoma cells were treated with tunicamycin (TM, 10  $\mu$ g/ml), DTT (2 mM) or both drugs for 6 h (Benedetti *et al.*, 2000). Blots were hybridized with probes specific for ERp44, actin and BiP, as indicated. Densitometric quantitations are reported on the right, and expressed as fold induction relative to untreated cells.

putative active site of the trx-like domain. Sequence conservation is striking in several regions, including the trx- and calsequestrin-like domains, as well as in two stretches rich in glutamic acids (239–288) and histidines (350–366). A KTEL sequence is found at the C-terminus of the *C.elegans* homologue (Vennema *et al.*, 1992). In *Saccharomyces cerevisiae*, the proteins with higher homology with ERp44 are Pdi1p and Eug1p, but identity is lower (~25%) and restricted to the trx-like domains.

#### **ERp44 transcripts are widely distributed and accumulate during the UPR**

ERp44 transcripts of ~1500 bases are present in all cell lines analysed so far (Figure 3A). Transcripts of ~2600 bases are also detectable, particularly in SK-N-BE neuroblastoma cells. This species probably originates from polyadenylation at the second cluster of AATAAA motifs in the ERp44 sequence (see Figure 1C). The ubiquitous expression of ERp44 was also suggested by virtual PCRs on expression databases, using LabOnWeb ([www.labonweb.com](http://www.labonweb.com))-assisted computational analysis (higher expression level in breast, brain and colon tissue extracts and cell lines). Similar results were reported for KIAA0573 in the HUGE Protein Database (Kazusa DNA Research Institute).

ER stress induces the transcription of many ER chaperones and enzymes (Lee, 2001). ERp44 transcripts accumulated in SK-N-BE cells following treatment with the UPR inducers tunicamycin and dithiothreitol (DTT) (Figure 3B) but not in other stress conditions, such as

serum deprivation or heat shock (not shown), indicating that ERp44 is a bona fide UPR gene. This is consistent with the presence of a CCAACN<sub>9</sub>CCCAG box upstream of the ERp44 ATG codon (see Figure 1C), similar to the ERSE present in the human PDI promoter (CCAACN<sub>9</sub>CCCCG) (Yoshida *et al.*, 1998).

#### **ERp44 is an ER resident protein**

The presence of a leader peptide and an RDEL motif suggests that ERp44 is a soluble resident protein of the ER lumen. In agreement with this, HA-tagged ERp44 largely colocalized in HeLa transfectants with calnexin (CNX) or PDI (Figure 4A). A polyclonal antiserum (B68) raised in rabbits against a GST–ERp44 fusion protein (see Materials and methods and Figure 5A below) yielded a similar staining pattern (not shown), confirming that endogenous ERp44 is also localized primarily in the ER.

After membrane partitioning, the majority of HA–ERp44 is found in the soluble fraction, where most endogenous PDI resides (Figure 4B). However, a considerable portion fractionates in the pellet, indicating that ERp44 might establish interactions with integral or peripheral membrane molecules (Pagani *et al.*, 2000).

#### **ERp44 binds covalently to both hEROs**

To confirm that ERp44 interacts covalently with hEROs, HeLa cells were cotransfected with HA–ERp44 and myc-tagged Ero1-L $\alpha$  or Ero1-L $\beta$  (Figure 4C). Clearly, Ero1-L $\alpha$  was coprecipitated by anti-HA antibodies (lane 1, lower panel); conversely, HA–ERp44 was coprecipitated by anti-myc (lane 5, upper panel). The interaction between Ero1-L $\alpha$  and ERp44 was mainly covalent, as bands of ~110 kDa were detected under non-reducing conditions with both anti-myc and anti-HA (lanes 2 and 6). Similarly, ERp44 was coprecipitated by anti-myc antibodies from cells co-expressing HA–ERp44 and Ero1-L $\beta$ –myc (lane 9). Coprecipitation required the simultaneous expression of both HA–ERp44 and Ero1-L $\alpha$ –myc or Ero1-L $\beta$ –myc (see MOCK lanes 3, 4, 7, 8 and 10). Spots of 44 kDa were found previously in mixed disulfides with both Ero1-L $\alpha$  and  $\beta$  by diagonal gels (Mezghrani *et al.*, 2001), suggesting that endogenous ERp44 covalently binds to both oxidoreductins. High molecular weight bands, probably corresponding to covalent complexes containing more than one copy of Ero1-L $\alpha$  and/or ERp44, are also labelled by anti-HA (lane 6), and anti-myc upon prolonged exposure (not shown, see also Figures 1A and 7). MS failed to detect additional proteins in these species, the stoichiometry of which remains to be determined. The most slowly migrating band labelled by anti-myc (Figure 4C, lower panel, lane 6) corresponds to the complex Ero1-L $\alpha$ –PDI mixed disulfides. Probing the blots with antibodies specific for PDI revealed that PDI coprecipitated with both Ero1-L $\alpha$  and Ero1-L $\beta$  (Benham *et al.*, 2000; Mezghrani *et al.*, 2001), but not with ERp44 (see Supplementary data available at *The EMBO Journal* Online). This further confirms the specificity of the interaction between ERp44 and hEROs.

#### **ERp44 forms covalent complexes with several endogenous proteins in HeLa cells**

The presence of ERp44 in the membrane-containing pellets (Figure 4B) indicated that it could interact with

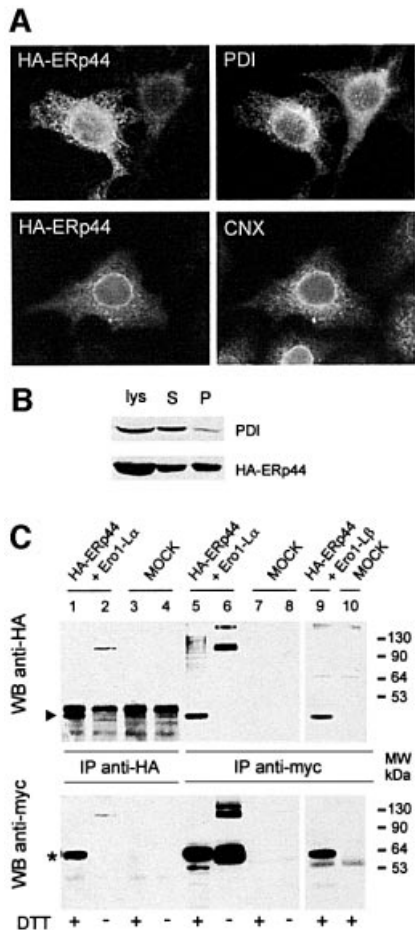


**Fig. 4.** ERp44 is a soluble ER resident protein forming mixed disulfides with both Ero1-L $\alpha$  and Ero1-L $\beta$ . (A) ERp44 colocalizes with ER markers. HeLa cells transfected with a plasmid driving the expression of HA-ERp44 were simultaneously stained with anti-HA (left panels, HA-ERp44) and either anti-PDI or anti-calnexin (CNX) and analysed by immunofluorescence. (B) Membrane partitioning of HA-ERp44. Soluble (S) and pelleted (P) proteins were resolved by SDS-PAGE under reducing conditions and transferred to nitrocellulose filters, which were hybridized with anti-PDI (top) or anti-HA-ERp44 (bottom) antibodies. (C) ERp44 forms mixed disulfides with both Ero1-L $\alpha$  and Ero1-L $\beta$ . HeLa cells were cotransfected with plasmids driving the expression of HA-ERp44 and either Ero1-L $\alpha$ -myc or Ero1-L $\beta$ -myc, or with empty vectors (MOCK). Lysates were immunoprecipitated with anti-HA or anti-myc. Blots were labelled with the antibodies indicated. The arrowhead and the asterisk indicate monomeric ERp44 and hEROs, respectively. The difference in intensity of the signal in lanes 1 and 2 (reduced and non-reduced, respectively) might be due to the formation of high molecular weight complexes and/or to technical artefacts such as different electrotransfer or epitope accessibility. The faster-migrating band stained by anti-myc (lane 5, bottom panel) might represent unglycosylated, untranslocated or proteolytically cleaved Ero1-L $\alpha$ , as it is also stained by D5 antibodies (Benham *et al.*, 2000).

membrane proteins. To investigate whether ERp44 forms mixed disulfides with additional endogenous molecules, HeLa cells were transfected with HA-tagged ERp44 or with an empty vector (Figure 5A). Under reducing conditions (lane 3) anti-ERp44 antibodies (B68) decorated a band of ~44 kDa in non-transfected HeLa cells. The mobility was slightly lower in transfected cells (lane 5), corresponding to the presence of an N-terminal HA tag. Under non-reducing conditions, monomeric ERp44

migrated more rapidly, suggesting the presence of intra-chain disulfide bonds (Figure 5A, lanes 4 and 6). The intensity of the band, however, was greatly reduced. Several bands of higher molecular weight were detected in both transfected and control HeLa cells, suggesting that both endogenous and exogenous ERp44 formed mixed disulfides with other proteins (see arrowheads on the right). Similar complexes including endogenous ERp44 were detectable also in SK cells (not shown). The proteins that are part of these complexes remain to be identified. To verify whether one of them might be endogenous Ero1-L $\alpha$ , the anti-HA immunoprecipitates from control or HA-ERp44-expressing cells were resolved under reducing or non-reducing conditions. D5 polyclonal antibodies labelled bands of ~110 kDa from HeLa cells expressing HA-ERp44, but not from untransfected cells (Figure 5B, compare lanes 1 and 2). Upon reduction, the D5 reactive band migrated with a mobility of 65 kDa, indistinguishable from that of transfected untagged Ero1-L $\alpha$  (lanes 5 and 6). Taken together, these findings indicated that HA-ERp44 can form mixed disulfides with endogenous Ero1-L $\alpha$ . Due to background problems, neither the presence nor the abundance of ERp44-Ero1-L $\alpha$  mixed disulfides in untransfected cells could be determined.

#### **ERp44 covalently binds both Ig-K and Ig-J chains, but with different kinetics**

To investigate whether ERp44 can bind to cargo proteins, HeLa cells were cotransfected with HA-ERp44 and either one of two different myc-tagged Ig subunits, K or J chains. The former is folding competent and is secreted by non-lymphoid cells. In contrast, JcM cannot assemble into transport competent Ig polymers in the absence of heavy and L chains, and they are therefore retained in the ER and eventually degraded by proteasomes (Mancini *et al.*, 2000).

To follow the interactions of the two cargo proteins with ERp44 and correlate them with their folding patterns, we employed a pulse-chase protocol described previously in detail (Mezghrani *et al.*, 2001). As is evident from the reducing gels, ERp44 interacts transiently with K chains, but more stably with JcM chains (compare lower panels in Figure 6A and B). Little JcM was coprecipitated by anti-HA antibodies immediately after the pulse (Figure 6B, time = 0 min, lower panel), when most J chains are entirely reduced (Mezghrani *et al.*, 2001). In contrast, some K chains were already coprecipitated at the end of the pulse (Figure 6A, lower panel). Some partially oxidized K chains were present at this time point (Mezghrani *et al.*, 2001), highlighting the easier folding of this transport-competent subunit.

Analyses under non-reducing conditions indicated that the binding between ERp44 and Ig subunits was mostly covalent (Figure 6A and B, upper panels). It is noteworthy that soon after the pulse with DTT, newly synthesized ERp44 was also mainly reduced (upper panels, time = 0). Even after 2 min of chase, intra-chain disulfide bonds were formed, as indicated by the electrophoretic shift. Also the cargo-ERp44 mixed disulfides underwent mobility shifts during the chase, suggesting that inter-chain bonding can precede the formation of some intra-molecular bridges. Taken together, these results indicate that ERp44 interacts

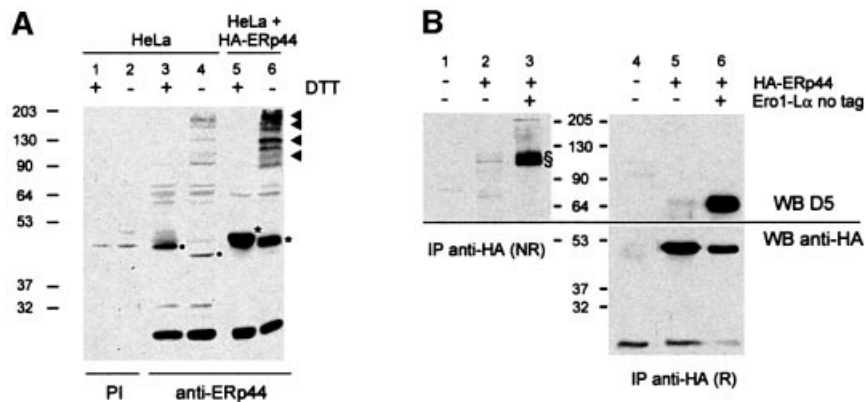


**Fig. 5.** ERp44-containing mixed disulfides in HeLa cells. (A) Lysates of HeLa cells, before (lanes 1–4) or 48 h after transfection with a plasmid driving the expression of HA-ERp44 (lanes 5 and 6), were resolved under reducing (+DTT) or non-reducing (–) conditions and transferred to a nitrocellulose filter, which was labelled with a polyclonal rabbit anti-GST-ERp44 antiserum (lanes 3–6) or with pre-immune serum (PI, lanes 1 and 2) as a control. The lysates of  $1.5 \times 10^5$  untransfected HeLa cells and of  $1 \times 10^5$  HA-ERp44-expressing cells were loaded. The different electrophoretic mobilities of the bands indicated by asterisks and dots indicate that both endogenous (lanes 3 and 4, dots) and exogenous ERp44 (lanes 5 and 6, asterisks) form intra-chain disulfide bonds. The presence of the HA tag in exogenous molecules explains their slower mobility with respect to endogenous ERp44. Arrowheads on the right hand margin point to ERp44-containing mixed disulfides. Whilst more abundant in transfected cells, these are detectable also in untransfected HeLa cells (lane 4). The band of ~26 kDa labelled by the GST-ERp44-specific antiserum might be endogenous GST. (B) Lysates of HeLa cells transfected as indicated were immunoprecipitated with immobilized anti-HA antibodies. Complexes were resolved under reducing (R) or non-reducing (NR) conditions and transferred to nitrocellulose. The blot shown on the right was cut horizontally and the upper and lower panels stained with D5 and anti-HA antibodies, respectively. Complexes including ERp44 and Ero1- $\alpha$  (endogenous or transfected) are indicated by §. Only one-third of the immunoprecipitated material was loaded on HA-ERp44+Ero1- $\alpha$  lanes.

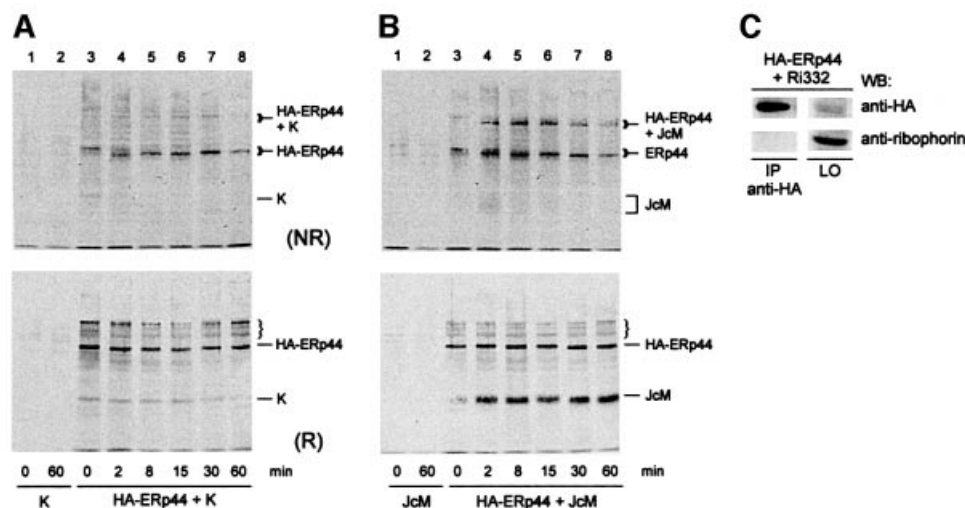


**Fig. 6.** ERp44 interacts with partially folded Ig subunits. HeLa cells were cotransfected with plasmids driving the expression of HA-ERp44 and myc-tagged Ig-K or J chains (K or JcM, respectively) or of a truncated ribophorin mutant (Ri332). (A) Transport-competent K chains interact transiently with ERp44. HeLa cells co-expressing HA-ERp44 and K chains were pulsed for 5 min with  $^{35}\text{S}$ -labelled amino acids in the presence of 3 mM DTT and chased for the times indicated without the reducing agent. Lysates were immunoprecipitated with anti-HA and resolved under non-reducing (NR, upper panel) or reducing (R, lower panel) conditions. The mobility of monomeric and ERp44-bonded K is indicated on the right hand margin. (B) JcM folding intermediates interact stably with ERp44. HeLa cells co-expressing HA-ERp44 and JcM were pulse-chased, immunoprecipitated and resolved as in (A). The bands indicated by the bracket are precipitated by anti-HA also from K-expressing cells (see A) and might correspond to endogenous ERp44 substrates. (C) A short-lived mutant ribophorin that lacks cysteine residues (Ri332) does not interact with ERp44. Lysates from HeLa cells co-expressing HA-ERp44 and Ri332 were immunoprecipitated with anti-HA. The immunoprecipitated material (IP) and 1/20 of that left over (LO) after immunoprecipitation were loaded on to the gel. Blots were hybridized with anti-HA or anti-ribophorin antibodies, as indicated.

preferentially with folding intermediates, mainly via inter-chain disulfides.

To determine whether ERp44 also binds to a misfolded protein that lacks cysteine residues, a truncated ribophorin mutant (Ri332), which, like JcM, is rapidly degraded by proteasomes (de Virgilio *et al.*, 1998) was co-expressed with ERp44 in HeLa cells. No Ri332 was coprecipitated

by anti-HA in conditions in which both JcM and K chains were bound (Figure 6C).

#### **ERp44 alters the redox state of Ero1- $\alpha$**

In all transfectants examined so far, two isoforms of Ero1- $\alpha$  (OX1 and OX2) can be detected, albeit in different relative amounts (Figure 7; Benham *et al.*, 2000;

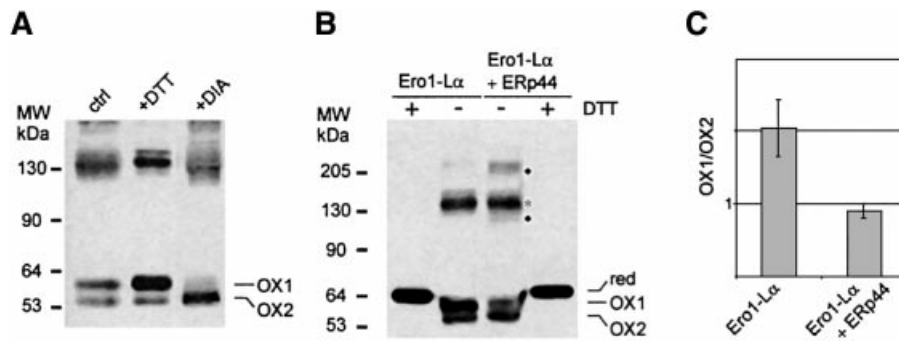


**Fig. 7.** Functional role of ERp44 in oxidative protein folding. (A) DTT and diamide alter the distribution of the different redox isoforms of Ero1-L $\alpha$  (OX1 and OX2). HeLa cells expressing myc-tagged Ero1-L $\alpha$  were treated for 5 min with 5 mM DTT or diamide (DIA) before lysis and electrophoresis under NR conditions. Western blots were labelled with anti-myc antibodies. (B) ERp44 overexpression favours the accumulation of OX2. HeLa cells expressing myc-tagged Ero1-L $\alpha$  alone or with HA-ERp44 were analysed by western blotting as in (A). Dots indicate bands containing only Ero1-L $\alpha$  and ERp44, while the asterisk indicates Ero1-L $\alpha$  and PDI complex. The 'smile' generated by lateral diffusion of the reducing agent between adjacent lanes underscores that OX1 and OX2 are redox isoforms. (C) OX1/OX2 ratios were calculated by densitometry in HeLa transfectants expressing Ero1-L $\alpha$  alone or with HA-ERp44. The average of four experiments and standard deviation are shown. The OX1/OX2 ratio changed slightly in different experiments depending on cell concentration and method of extraction. However, it was consistently lower in cells overexpressing ERp44 than in matched controls.

Mezghrani *et al.*, 2001). OX1 and OX2 display different susceptibilities to proteases (F.Talamo, T.Anelli, M.Alessio, R.Sitia and A.Bachi, unpublished results), suggesting that they represent different structural conformers. Membrane-permeant oxidants or reducing agents affected the OX1/OX2 ratio (Figure 7A). OX1 prevailed when HeLa transfectants were exposed to DTT, whilst diamide induced the accumulation of OX2. These changes were reversible, as the OX1/OX2 ratios were restored upon further culture without the drugs (not shown). These observations confirmed that OX1 and OX2 are redox isoforms, possibly representing different conformers in the Ero1-L $\alpha$  functional cycle. The overexpression of ERp44 altered the relative amounts of the two isoforms, shifting the equilibrium towards OX2 (Figure 7B and C).

## Discussion

By transferring electrons from PDI to unknown acceptor(s), hEROs play a key role in controlling the redox state in the ER (Mezghrani *et al.*, 2001). Growth of the yeast *ero1-1* mutant strain can be partially restored by diamide (Cuozzo and Kaiser, 1999), suggesting that the primary function of Ero1 proteins is to generate oxidizing conditions in the ER. However, in this organelle disulfide bonds are not only formed but also isomerized (Debarbieux and Beckwith, 1999; Noiva, 1999) and, in the case of terminally unfolded polypeptides destined for proteasomal degradation, reduced before the dislocation to the cytosol (Fagioli *et al.*, 2001). By selectively interacting with oxidoreductases, Ero1 molecules might precisely deliver oxidizing equivalents, allowing formation, isomerization and reduction of disulfides to take place simultaneously in the same compartment.

### **ERp44, a novel member of the thioredoxin family residing in the ER**

With the aim of dissecting the molecular machines involved in ER redox control, we decided to isolate and characterize proteins that, in addition to PDI (Benham

*et al.*, 2000; Mezghrani *et al.*, 2001), form mixed disulfides with hEROs in HeLa cells. Amongst these, the most abundant was a protein of ~44 kDa, which we named ERp44.

Its sequence reveals many of the features of a molecule possibly involved in the control of oxidative protein folding in the ER. The combination of a cleaved N-terminal signal sequence with a C-terminal RDEL tetrapeptide explains its main localization in the ER (Figure 4A). Subcellular fractionation assays reveal that, whilst most PDI is localized in the soluble fraction, a considerable proportion of ERp44 is found in the pellet (Figure 4B). Similar behaviour was also observed for both Ero1-L $\alpha$  and -L $\beta$  (Pagani *et al.*, 2000), which, like ERp44, do not have hydrophobic stretches capable of mediating membrane insertion following cleavage of the leader peptide. It is likely that ERp44 establishes interactions with integral or peripheral membrane proteins.

Soon after the signal peptide, a trx-like domain is encountered. Computer modelling predicts a structure that can be largely superimposed on the active domains of PDI. There are important differences, however. The second cysteine of the CXXC motif characteristic of most oxidoreductases is replaced by a serine. The CRFS motif and the surrounding sequences are extremely conserved in all species (Figure 2), suggesting an important functional role for this region (Debarbieux and Beckwith, 1999; Norgaard and Winther, 2001). Indeed, MS analyses indicate that the cysteine of the CRFS motif is involved in the formation of mixed disulfides with Ero1-L $\alpha$  (F.Talamo and A.Bachi, unpublished observations). Unlike trx or PDI, the N-terminal domain of ERp44 contains an additional cysteine at position 63 in the mature protein. Structural modelling predicts this additional cysteine to be localized in a loop juxtaposed to the CRFS motif, but the potential relevance of this residue remains to be established. In *S.cerevisiae*, the proteins with the highest similarities to ERp44 are Eug1p and Pdi1p. Also, Eug1p contains, in its two active trx-like domains, a CXXS motif followed by a cysteine in a position similar to

Cys63 in ERp44. However, the surrounding sequences, extremely conserved in the ERp44 subfamily (Figure 2), are rather divergent in Eug1p. It will be of interest to determine whether ERp44 can complement yeast mutants that are deficient in ER oxidoreductases (Norgaard *et al.*, 2001).

The trx-like domain is followed by a 62 amino acid region with similarities to the second domain of calnextrin. The rest of the protein shows no obvious sequence similarities with other known protein families, even though it contains two extremely conserved regions, rich in glutamic acids and histidines, respectively.

### **ERp44 is induced during ER stress**

Like many ER folding factors, ERp44 transcripts are induced by agents that cause the accumulation of unfolded proteins in the ER. The sensitivity to ER stress correlates with the presence of an ERSE sequence (Mori *et al.*, 1998) in the 5' region of the gene (Figure 1C). The observation that ERp44 is induced to a lesser extent than BiP (Figure 3B) might reflect the presence of a single ERSE box in the regulatory region. Proteomic analyses revealed that ERp44 increases during B-lymphocyte plasma cell differentiation with kinetics similar to other ER chaperones and enzymes (E.vanAnken, R.Sitia and I.Braakman, unpublished observations), paralleling the massive development of the ER and Ig secretion.

Analysis of the available ESTs reveals some polymorphisms in ERp44, involving Pro243, Pro262 and Gln312. It will be interesting to determine whether these polymorphisms have any functional or pathological correlations, particularly for diseases related to protein misfolding or accumulation (Kopito and Ron, 2000; Sherman and Goldberg, 2001).

### **Functional role of ERp44**

Owing to the absence of the downstream cysteine in the active motif, ERp44 is not likely to be very effective as an oxidase or a reductase. Therefore, ERp44 does not appear to be the long sought electron acceptor located upstream of hEROs in the pathway of disulfide bond formation. Hence, what is its role? ERp44 interacts not only with hEROs, but also with other proteins. The interaction is transient with K chains, which rapidly acquire transport competence, but more stable with unassembled J chains, which undergo retention and redox-sensitive proteasomal degradation (Mancini *et al.*, 2000). The rate of JcM degradation, however, is not increased in cells overexpressing ERp44 (see Supplementary data).

It is noteworthy that ERp44 does not interact with a truncated ribophorin mutant (Ri332), which like J is a substrate of ER-associated degradation but lacks cysteine residues (de Virgilio *et al.*, 1998). Taken together, the results shown in Figures 4C and 6 indicate that ERp44 interacts with intermediates in the pathways of oxidative folding, mainly through the formation of inter-chain disulfide bonds. Some monomeric K and J chains are initially co-immunoprecipitated by anti-HA (Figure 6A and B, upper panels), indicating that ERp44 can also bind non-covalently to substrates. This initial binding may be stabilized by the formation of a covalent bond. This might explain why little if any truncated ribophorin could be found associated with ERp44. It is also possible that

ERp44 interacts specifically with defined class(es) of substrate. The kinetics and specificity of the interactions with different client molecules indicate that ERp44 is a folding assistant. Due to the presence of a single cysteine in its active motif, ERp44 may act as an isomerase (Debarbieux and Beckwith, 1999). It might also contribute to the retention of molecules with exposed thiols (Alberini *et al.*, 1990; Sitia *et al.*, 1990; Isidoro *et al.*, 1996).

### **Why does ERp44 bind to hEROs?**

In cells overexpressing Ero1-L $\alpha$ , the vast majority of ERp44 is found in mixed disulfides with the oxidoreductin (Figure 4C). The abundance of cysteine residues can make Ero1-L $\alpha$  a privileged substrate of ERp44. Binding of ERp44 to Ero1-L $\alpha$  might have physiological consequences. We have shown previously that Ero1-L $\alpha$  exists in distinct redox isoforms (Benham *et al.*, 2000) whose relative abundance is reversibly changed by redox perturbants (Figure 7A). DTT and diamide have opposite effects, favouring the accumulation of OX1 and OX2, respectively. The reversibility of these changes suggests that cells can efficiently regulate the OX1/OX2 ratios. Although their exact functional role(s) remain to be established, OX1 and OX2 might reflect functional statuses of the Ero1-L $\alpha$  working cycle. Particularly in professional secretory cells, mechanisms probably exist that favour the interaction of oxidized hEROs with reduced PDI, and facilitate the detachment of the hERO-PDI complexes once the disulfide bond has been transferred to PDI. The slower mobility of OX1 suggests that this isoform is less compact than OX2, a feature that might favour the binding of reduced PDI (Tsai *et al.*, 2001). As determined by trypsin sensitivity assays, it is mostly the OX1 form that is found in complexes with PDI and ERp44 (F.Talamo, T.Anelli, M.Alessio, R.Sitia and A.Bachi, unpublished results).

By favouring the accumulation of OX2, ERp44 may play an important role in controlling the function of hEROs and hence the redox state of the ER. It remains to be established whether the shift in the OX1/OX2 ratios is induced only by the selective sequestration of OX1 in covalent complexes, or also by catalysed isomerization. Whatever the mechanism involved, the different availability of monomeric Ero1-L $\alpha$  isoforms might have an impact on the downstream components in the pathway.

## **Materials and methods**

### **Cells and reagents**

Cell lines were obtained from ATCC. DTT, *N*-ethylmaleimide (NEM), iodoacetamide (IAA), trypsin, NP-40, SDS, Coomassie Blue colloidal were from Sigma Chemical Co (St Louis, MO); fetal calf serum (FCS) and culture media from Gibco-BRL (Milan, Italy); Sepharose-conjugated proteins A and G, CNBr-activated Sepharose and ECL reagents from Amersham-Pharmacia (Uppsala, Sweden). Horseradish peroxidase goat anti-mouse Ig was from Southern Biotechnology Associates, Inc (Birmingham, AL); Alexa-green goat anti-mouse Ig and Alexa-red goat anti-rabbit Ig from Molecular Probes, (Leiden, NL). Mouse monoclonal antibodies specific for myc and HA (9E10 and 12CA5, respectively) were used to precipitate tagged molecules. Rabbit antibodies against calnexin, PDI and Ero1-L $\alpha$  were generously made available by M.Molinari (IRB, Bellinzona, Switzerland), I.Braakman (Utrecht University, The Netherlands) and A.Benham (Durham, UK).

Polyclonal antibodies (B68) were generated by immunizing rabbits (Primm SpA, Milan, Italy) with a GST-ERp44 fusion protein (see below), purified on glutathione-Sepharose (Amersham-Pharmacia).

### Plasmids and vectors

ERp44 cDNAs were obtained by PCR on the RT products from HeLa and SK-N-BE cells, using oligos TAS and TAR (see below) flanking the open reading frame. The PCR product was inserted in pGEM-Teasy (Promega) and sequenced (Primm SpA).

A tagged version of ERp44 was generated by inserting an HA tag (YPYDVPDYA) after the leader sequence cleavage site (Figure 1B). A glutamic acid was inserted before the tag to recreate the endogenous cleavage site. This construct was obtained by sequential PCR on plasmid pBSK+II KIAA0573 (made available by Kazusa DNA Research Institute), using primers TA1R/TA2S and TA3S/TA4R (see below) in the first reactions and TA2S/TA4R in the second.

The PCR product was inserted into pGEM-Teasy, cleaved using the introduced *Xho*I and *Acc*65I sites and inserted into pcDNA3.1–(Stratagene). To generate GST–ERp44, *Bam*HI and *Not*I sites were inserted at the N- and C-termini of ERp44, respectively, using primers TA5S and TA6R. The PCR product was inserted into pGEX-4T-1 (Amersham-Pharmacia). The resulting construct was used to transform *Escherichia coli* BL21. Expression of the fusion protein was induced by IPTG. Primers are: TAS (GCCGCTGCCTGGAGAATCCTC); TAR (CCACCACGTAGGTTGATGCTG); TA1R (GCGTAGTCAGGCA-CATCATACGGATATTCAGTTGTTACAGGAGTAAAAAC); TA2S (CAACTCGAGCGTTACCATGCATCCTGGCC); TA3S (TATCCGTAT-GATGTGCCTGACTACGCCGAAATAACAAGTCTTGATACAGAG-AATATAG); TA4R (TTTGGTACCTTAAAGCTCATCTCGATCCCT-CAATAG); TA5S (CGCAGCGGATCCGAAATAACAAGTCTTG-ATACAG); TA6R (CGTTGCGGCCGCTCATTTTTAAAGTCCATCT-CGATCC).

### Transfection, immunofluorescence, pulse-chase, immunoprecipitation and western blotting

Transient transfection and immunofluorescence were performed as described (Pagani *et al.*, 2000; Mezghrani *et al.*, 2001). Cells were detached by trypsinization, washed once in ice-cold phosphate-buffered saline (PBS) and incubated for 5 min with 10 mM NEM to block disulfide interchange. Cells were then lysed in RIPA buffer (150 mM NaCl, 1% NP-40, 0.1% SDS, 50 mM Tris–HCl pH 8.0) containing 10 mM NEM. Cells were pulsed with [<sup>35</sup>S]amino acids for 5 min with or without 5 mM DTT, washed and chased for different lengths of time as described (Mezghrani *et al.*, 2001). At the end of each chase time cells were treated with 10 mM NEM and lysed as above. Lysates were immunoprecipitated with the appropriate antibody (anti-myc 9E10, anti-HA 12CA5) cross-linked to protein G or protein A–Sepharose beads (Reddy *et al.*, 1996). The beads were washed in 0.5 M NaCl, 0.5% SDS, 10 mM Tris–HCl pH 7.5, eluted in Laemmli buffer and resolved by SDS–PAGE. Gels were stained with Coomassie Blue colloidal, or either processed for fluorography or transferred to nitrocellulose filters for ECL. Relevant bands were quantified by densitometry.

Subcellular fractionation was performed as in Gruarin *et al.* (2000).

### MALDI and NanoES mass spectrometry

Bands of interest were excised from Coomassie-stained gels, digested overnight with trypsin and eluted as described (Shevchenko *et al.*, 1996). Aliquots of 1 µl were used for MALDI analysis. Alternatively, gel fragments were further extracted and the resulting peptide mixture subjected to a single desalting/concentration step before mass spectrometric analysis over µZipTip C<sub>18</sub> (Millipore Corporation, Bedford, MA) or POROS R2 material (Applied Biosystems, Framingham, MA).

Dried protein digests were dissolved in 5% formic acid and 1 µl was loaded on to the MALDI target using the dried droplet technique and α-cyano-4-hydroxycinnamic acid (HCCA) as matrix. MALDI mass spectra were obtained on a Voyager-DE STR (Applied Biosystems) time-of-flight (TOF) mass spectrometer and processed via the Data Explorer software. Proteins were unambiguously identified by searching a comprehensive non-redundant protein database using the program ProFound (Zhang and Chait, 2000). The remaining 90% of the protein digest was then concentrated and desalted over a capillary column packed manually with 200 nl of POROS R2 material conditioned with 5% formic acid. The peptide mixture was eluted using 1 µl of 50% methanol/5% formic acid directly into the electrospray needle (Protana, Denmark).

NanoES was performed on a Q-Star Pulsar (QqTOF hybrid system from PE SCIEX Instruments, Toronto, Canada). Multiply charged peptides were fragmented in order to produce peptide sequence tags. The tags were then screened against a non-redundant database containing >600 000 entries, using the PeptideSearch software (Wilm *et al.*, 1996). No limitations were imposed on protein molecular weight and species of origin.

### mRNA expression, tissue distribution and UPR induction

UPR induction, total cellular RNA preparations and northern blot analyses were performed as described previously (Benedetti *et al.*, 2000). An *Ssp*I fragment (550–833 from the ATG start codon) was used as a probe for ERp44.

### Supplementary data

Supplementary data for this paper are available at *The EMBO Journal* Online.

### Acknowledgements

We thank Cristina Benedetti, Adam Benham, Gloria Bertoli, Ineke Braakman, Neil Bulleid, Giorgio Casari, Giacomo Consalez, Maddalena de Virgilio, Claudio Fagioli, Anna Fassio, Erwin Ivessa, Maurizio Molinari, Raffaella Scorza and Eelco vanAnken for helpful reagents, suggestions and discussions, and Stefania Trinca for secretarial assistance. This work was supported in part through grants from the Associazione Italiana per la Ricerca sul Cancro (AIRC), Consiglio Nazionale Ricerche (CNR, PF BioTec 00123; 5% BioTec 00089/00017) and Telethon to R.S. T.A., A.M. and T.S. are recipients of fellowships from the Gruppo Italiano Lotta alla Scleroderma, the European Community (CEE52106) and Telethon (380/bs), respectively.

### References

- Alberini, C.M., Bet, P., Milstein, C. and Sitia, R. (1990) Secretion of immunoglobulin M assembly intermediates in the presence of reducing agents. *Nature*, **347**, 485–487.
- Andres, D.A., Dickerson, I.M. and Dixon, J.E. (1990) Variants of the carboxyl-terminal KDEL sequence direct intracellular retention. *J. Biol. Chem.*, **265**, 5952–5955.
- Benedetti, C., Fabbri, M., Sitia, R. and Cabibbo, A. (2000) Aspects of gene regulation during the UPR in human cells. *Biochem. Biophys. Res. Commun.*, **278**, 530–536.
- Benham, A.M., Cabibbo, A., Fassio, A., Bulleid, N., Sitia, R. and Braakman, I. (2000) The CXXCXXC motif determines the folding, structure and stability of human Ero1-L $\alpha$ . *EMBO J.*, **19**, 4493–4502.
- Bulleid, N.J. and Freedman, R.B. (1988) Defective co-translational formation of disulphide bonds in protein disulphide-isomerase-deficient microsomes. *Nature*, **335**, 649–651.
- Cabibbo, A., Pagani, M., Fabbri, M., Rocchi, M., Farmery, M.R., Bulleid, N.J. and Sitia, R. (2000) Ero1-L, a human protein that favors disulfide bond formation in the endoplasmic reticulum. *J. Biol. Chem.*, **275**, 4827–4833.
- Cuozzo, J.W. and Kaiser, C.A. (1999) Competition between glutathione and protein thiols for disulphide-bond formation. *Nature Cell Biol.*, **1**, 130–135.
- Debarbieux, L. and Beckwith, J. (1999) Electron avenue: pathways of disulfide bond formation and isomerization. *Cell*, **99**, 117–119.
- de Virgilio, M., Weninger, H. and Ivessa, N.E. (1998) Ubiquitination is required for the retro-translocation of a short-lived luminal endoplasmic reticulum glycoprotein to the cytosol for degradation by the proteasome. *J. Biol. Chem.*, **273**, 9734–9743.
- Ellgaard, L., Molinari, M. and Helenius, A. (1999) Setting the standards: quality control in the secretory pathway. *Science*, **286**, 1882–1888.
- Fagioli, C., Mezghrani, A. and Sitia, R. (2001) Reduction of inter-chain disulfide bonds precedes the dislocation of Ig- $\mu$  chains from the endoplasmic reticulum to the cytosol for proteasomal degradation. *J. Biol. Chem.*, **276**, 40962–40967.
- Frاند, A.R. and Kaiser, C.A. (1999) Ero1p oxidizes protein disulfide isomerase in a pathway for disulfide bond formation in the endoplasmic reticulum. *Mol. Cell*, **4**, 469–477.
- Frاند, A.R., Cuozzo, J.W. and Kaiser, C.A. (2000) Pathways for protein disulphide bond formation. *Trends Cell Biol.*, **10**, 203–210.
- Gruarin, P., Thorne, R.F., Dorahy, D.J., Burns, G.F., Sitia, R. and Alessio, M. (2000) CD36 is a ditopic glycoprotein with the N-terminal domain implicated in intracellular transport. *Biochem. Biophys. Res. Commun.*, **275**, 446–454.
- Guex, N. and Peitsch, M.C. (1997) SWISS-MODEL and the Swiss-PdbViewer: an environment for comparative protein modeling. *Electrophoresis*, **18**, 2714–2723.
- Isidoro, C., Maggioni, C., Demoz, M., Pizzagalli, A., Fra, A.M. and Sitia, R. (1996) Exposed thiols confer localization in the endoplasmic

- reticulum by retention rather than retrieval. *J. Biol. Chem.*, **271**, 26138–26142.
- Klausner,R.D. and Sitia,R. (1990) Protein degradation in the endoplasmic reticulum. *Cell*, **62**, 611–614.
- Kohno,K., Normington,K., Sambrook,J., Gething,M.J. and Mori,K. (1993) The promoter region of the yeast KAR2 (BiP) gene contains a regulatory domain that responds to the presence of unfolded proteins in the endoplasmic reticulum. *Mol. Cell. Biol.*, **13**, 877–890.
- Kopito,R.R. (1997) ER quality control: the cytoplasmic connection. *Cell*, **88**, 427–430.
- Kopito,R.R. and Ron,D. (2000) Conformational disease. *Nature Cell Biol.*, **2**, E207–E209.
- Kozak,M. (1997) Recognition of AUG and alternative initiator codons is augmented by G in position +4 but is not generally affected by the nucleotides in positions +5 and +6. *EMBO J.*, **16**, 2482–2492.
- Lee,A.S. (2001) The glucose-regulated proteins: stress induction and clinical applications. *Trends Biochem. Sci.*, **26**, 504–510.
- Mancini,R., Fagioli,C., Fra,A.M., Maggioni,C. and Sitia,R. (2000) Degradation of unassembled soluble Ig subunits by cytosolic proteasomes: evidence that retrotranslocation and degradation are coupled events. *FASEB J.*, **14**, 769–778.
- Mezghrani,A., Fassio,A., Benham,A., Simmen,T., Braakman,I. and Sitia,R. (2001) Manipulation of oxidative protein folding and PDI redox state in mammalian cells. *EMBO J.*, **20**, 6288–6296.
- Molinari,M. and Helenius,A. (1999) Glycoproteins form mixed disulphides with oxidoreductases during folding in living cells. *Nature*, **402**, 90–93.
- Mori,K. (2000) Tripartite management of unfolded proteins in the endoplasmic reticulum. *Cell*, **101**, 451–454.
- Mori,K., Ogawa,N., Kawahara,T., Yanagi,H. and Yura,T. (1998) Palindrome with spacer of one nucleotide is characteristic of the *cis*-acting unfolded protein response element in *Saccharomyces cerevisiae*. *J. Biol. Chem.*, **273**, 9912–9920.
- Nielsen,H., Engelbrecht,J., Brunak,S. and von Heijne,G. (1997) Identification of prokaryotic and eukaryotic signal peptides and prediction of their cleavage sites. *Protein Eng.*, **10**, 1–6.
- Noiva,R. (1999) Protein disulfide isomerase: the multifunctional redox chaperone of the endoplasmic reticulum. *Semin. Cell Dev. Biol.*, **10**, 481–493.
- Norgaard,P. and Winther,J.R. (2001) Mutation of yeast Eug1p CXXS active sites to CXXC results in a dramatic increase in protein disulphide isomerase activity. *Biochem. J.*, **358**, 269–274.
- Norgaard,P., Westphal,V., Tachibana,C., Alsoe,L., Holst,B. and Winther,J.R. (2001) Functional differences in yeast protein disulfide isomerases. *J. Cell Biol.*, **152**, 553–562.
- Pagani,M., Fabri,M., Benedetti,C., Fassio,A., Pilati,S., Bulleid,N.J., Cabibbo,A. and Sitia,R. (2000) Endoplasmic reticulum oxidoreductin 1- $\beta$  (ERO1-L $\beta$ ), a human gene induced in the course of the unfolded protein response. *J. Biol. Chem.*, **275**, 23685–23692.
- Reddy,P., Sparvoli,A., Fagioli,C., Fassina,G. and Sitia,R. (1996) Formation of reversible disulfide bonds with the protein matrix of the endoplasmic reticulum correlates with the retention of unassembled Ig light chains. *EMBO J.*, **15**, 2077–2085.
- Roy,B. and Lee,A.S. (1999) The mammalian endoplasmic reticulum stress response element consists of an evolutionarily conserved tripartite structure and interacts with a novel stress-inducible complex. *Nucleic Acids Res.*, **27**, 1437–1443.
- Sherman,M.Y. and Goldberg,A.L. (2001) Cellular defenses against unfolded proteins: a cell biologist thinks about neurodegenerative diseases. *Neuron*, **29**, 15–32.
- Shevchenko,A., Wilm,M., Vorm,O. and Mann,M. (1996) Mass spectrometric sequencing of proteins silver-stained polyacrylamide gels. *Anal. Chem.*, **68**, 850–858.
- Sitia,R., Neuberger,M., Alberini,C., Bet,P., Fra,A., Valetti,C., Williams,G. and Milstein,C. (1990) Developmental regulation of IgM secretion: the role of the carboxy-terminal cysteine. *Cell*, **60**, 781–790.
- Tortorella,D., Story,C.M., Huppa,J.B., Wiertz,E., Jones,T.R. and Ploegh,H.L. (1998) Dislocation of type I membrane proteins from the ER to the cytosol is sensitive to changes in redox potential. *J. Cell Biol.*, **142**, 365–376.
- Travers,K.J., Patil,C.K., Wodicka,L., Lockhart,D.J., Weissman,J.S. and Walter,P. (2000) Functional and genomic analyses reveal an essential coordination between the unfolded protein response and ER-associated degradation. *Cell*, **101**, 249–258.
- Tsai,B., Rodighiero,C., Lencer,W.I. and Rapoport,T.A. (2001) Protein disulfide isomerase acts as a redox-dependent chaperone to unfold cholera toxin. *Cell*, **104**, 937–948.
- Tu,B.P., Ho-Schleyer,S.C., Travers,K.J. and Weissman,J.S. (2000) Biochemical basis of oxidative protein folding in the endoplasmic reticulum. *Science*, **290**, 1571–1574.
- Vennema,H., Heijnen,L., Rottier,P.J., Horzinek,M.C. and Spaan,W.J. (1992) A novel glycoprotein of feline infectious peritonitis coronavirus contains a KDEL-like endoplasmic reticulum retention signal. *J. Virol.*, **66**, 4951–4956.
- von Heijne,G. (1989) Control of topology and mode of assembly of a polytopic membrane protein by positively charged residues. *Nature*, **341**, 456–458.
- Wilm,M., Shevchenko,A., Houthaeve,T., Breit,S., Schweigerer,L., Fotsis,T. and Mann,M. (1996) Femtomole sequencing of proteins from polyacrylamide gels by nano-electrospray mass spectrometry. *Nature*, **379**, 466–469.
- Yoshida,H., Haze,K., Yanagi,H., Yura,T. and Mori,K. (1998) Identification of the *cis*-acting endoplasmic reticulum stress response element responsible for transcriptional induction of mammalian glucose-regulated proteins. Involvement of basic leucine zipper transcription factors. *J. Biol. Chem.*, **273**, 33741–33749.
- Zhang,W. and Chait,B.T. (2000) ProFound: an expert system for protein identification using mass spectrometric peptide mapping information. *Anal. Chem.*, **72**, 2482–2489.

Received October 12, 2001; revised December 14, 2001;  
accepted January 7, 2002